



## **Sabang Submarine Volcano Aceh, Indonesia: Review of Some Trace and Rare Earth Elements Abundances Produced by Seafloor Fumarole Activities**

HANANTO KURNIO<sup>1,2</sup>, ILDREM SYAFRI<sup>2</sup>, ADJAT SUDRADJAT<sup>2</sup>, and MEGA FATIMAH ROSANA<sup>2</sup>

<sup>1</sup>Marine Geological Institute, Research and Development Agencies for Energy and Mineral Resources  
Jln. Dr. Djunjunan No. 236, Bandung

<sup>2</sup>Faculty of Geology, Padjadjaran University  
Jln. Raya Bandung - Sumedang Km, 21, Jatinangor, Sumedang, Indonesia

Corresponding author: [hanantokurniosalamun@gmail.com](mailto:hanantokurniosalamun@gmail.com)

Manuscript received: October 10, 2015; revised: April 12, 2016;  
approved: October 27, 2016; available online: November 14, 2016

**Abstract** - Geochemical analyses of selected coastal and seafloor samples from Sabang Area revealed abundances of trace and rare earth elements. The selected samples of element abundances were mostly taken from seafloor in the vicinities of active fumaroles either by grab sampler operated from survey boat above fumarole point or by diver directly took the samples on the seafloor especially at Serui - Sabang Bay. Results show that samples closed to seafloor fumaroles demonstrate plenty of trace and rare earth elements. The trace and rare earth elements mean values (n=10) are: Nb (4.33 ppm), La (16.52 ppm), Ce (38.82 ppm), Nd (19.15 ppm), Ce (38.82 ppm), Pr (4.907 ppm), Nd (19.15 ppm), Sm (4.04 ppm), Gd (3.95 ppm), Dy (3.38 ppm), Th (6.432 ppm), and U (4.335 ppm). Negatively, statistical correlations between Fe, Zn, and Ni as the main sulphide elements with sulphur is interpreted that sulphide minerals do not form in the Sabang Sea. Sea water influence in the mineralization process was shown by the good correlations between Fe, Zn, Pb, Ni, and Ba.

**Keywords:** trace and rare earth elements, seafloor fumarole activities, Sabang, Aceh, Indonesia

© IJOG - 2016. All right reserved

### **How to cite this article:**

Kurnio, H., SYAFRI, I., SUDRADJAT, A., and ROSANA, M.F., 2016. Sabang Submarine Volcano Aceh, Indonesia: Review of Some Trace and Rare Earth Elements Abundances Produced by Seafloor Fumarole Activities. *Indonesian Journal on Geoscience*, 3 (3), p.173-183. DOI: [10.17014/ijog.3.3.173-183](https://doi.org/10.17014/ijog.3.3.173-183)

### **INTRODUCTION**

Sabang is a city located in Weh Island, Aceh - the northwesternmost province of Indonesian Territory (Figure 1). The city itself is located at the northern part, but administratively the whole island belongs to Sabang territory. This includes mountainous area covered by dense forest in the west, central, and southwest of the island.

The mountainous area shows a belt of volcanic cones observed from three dimensions terrain earthgoogle as well as from field works. Two belt

orientations are recognized within southeast - northwest and south - north direction. It seems that the volcanic belt reveals an active volcanism in Weh Island and surrounding waters.

Surface volcanisms are observed in the middle of Sabang Island at shallow coastal waters of Serui and Pria Laot as well as at its coastal zone. The activities take the form of fumaroles, solfataras, hot mud pool, hot ground, hot spring, and gas bubbles in water column above seafloor vent.

A number of scientists (*e.g.*, Heinrich *et al.*, 1999; William-Jones *et al.*, 2002; and Gilbert and

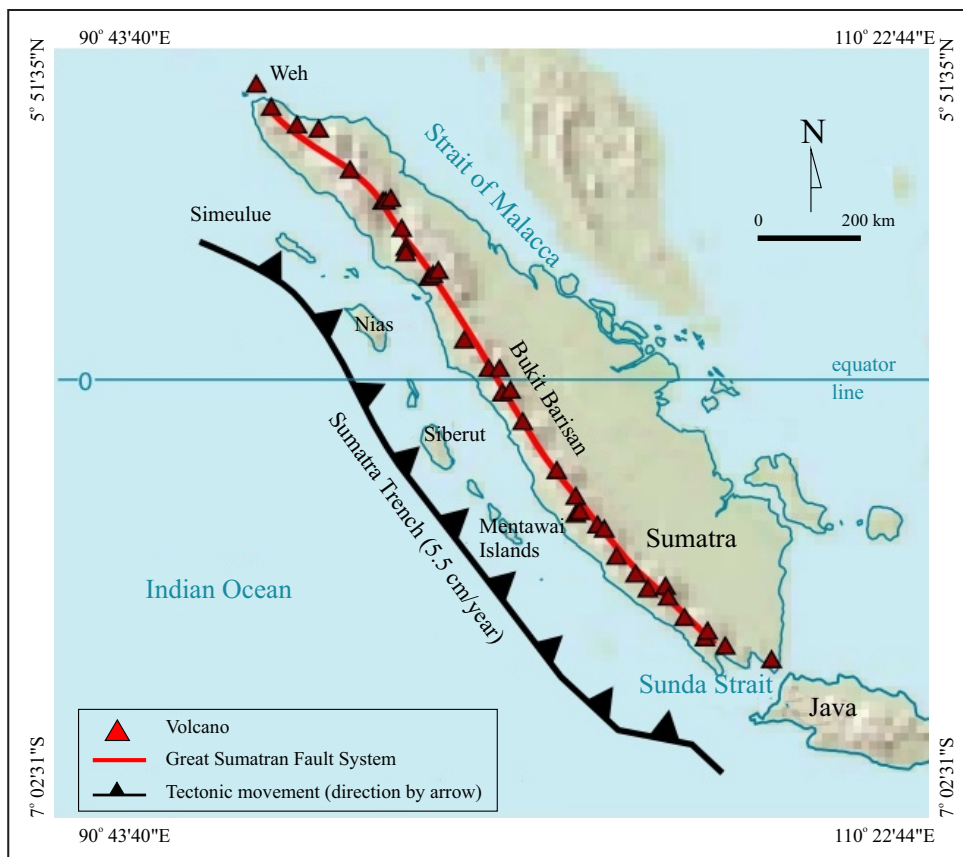


Figure 1. Location of Weh Island in volcanic belt of Sumatra which is incorporated by Great Sumatran Fault above subducted Indo-Australia Oceanic Plate (Source: Simoes *et al.*, 2004).

Williams-Jones, 2008) suggested that there were common trace and rare earth elements deposited in the vicinities of active volcanoes. However, the mechanism of that element occurrences might be discussed for a better understanding of whether or not those elements could become together in association one to another.

This paper presents and discusses geochemical, including trace and rare earth elements, data of the rocks and sediments from the Sabang Submarine Volcano, Aceh. The discussion is focused on how such elements deposited closed to the volcano. Marine geological and geophysical researches as well as statistical analyses have been done to better understand such relationship.

### REGIONAL GEOLOGY

Geology of Weh Island is largely influenced by the Great Sumatran Fault or simply Sumatran

Fault (Curry *et al.*, 1979; Bellier and Sebrier, 1994; Sieh and Natawidjaja, 2000; Dirasutisna and Hasan, 2005; Suhanto *et al.*, 2005; Barber *et al.*, 2005; Crow and Barber, 2005; and Curry, 2005). At the northern part of Sumatra, the fault is separated into two segments: Banda Aceh and Seulimeum (Sieh and Natawidjaja, 2000). The Banda Aceh segment is running at west side of the capital city of Aceh Province which is not active, while the active segment - Seulimeum continues to Weh Island. The combination of active fault and active volcano arrange the geology of Weh Island, and the island volcano belongs to Sunda volcanic belt which runs through the length of Sumatra (Tikoff, 1998). Regional marine geological and geophysical mapping had been conducted by MGI (Marine Geological Institute of Indonesia) in 2011 (Tim Geomarin I, 2011). The survey had identified the continuation of Sumatran Fault below the seafloor in the seismic record - south of Weh Island.

To understand the geology of the island, caldera collapse concept developed by Lagmay *et al.* (2000) was used. There are three collapse models, *i.e.* (a) a collapse model perpendicular to compressive regional main stress, (b) a collapse model perpendicular to normal fault, and (c) a collapse model influenced by transform fault with movement parallel with the fault (Figure 2).

The study area is interpreted to resemble the c model as it is influenced by Sumatra transform fault, and the collapse model is manifested by formation of calderas in the northwest and southeast of Weh, parallel with fault movement to those directions which nowadays are recognized as Sabang Bay and Balohan Bay (Figure 3).

The model is also important to explain the direction of magma progress. It tends to move to the collapse area. There are two areas as mentioned above, which nowadays are observed as the most active volcanic activities. The caldera collapse is an important aspect for hydrothermal fluids, because it acts as a conduit for the fluids reaching the surface.

## METHODS

Marine geology and geophysics were used to acquire the data. The marine geology includes seafloor sediment and rock samplings either by grab sampler or diver. The sampling was also conducted at coastal zone, especially at the most

active volcanism area in Serui and Pria Laot, in the middle of studied area.

The marine geophysical method used was shallow penetration single channel seismics, aiming to map the distribution of seafloor active or non-active fumaroles. Some interesting seafloor features were revealed from seismic survey.

The geochemical analyses used is an inductively coupled plasma atomic emission spectroscopy (ICP-AES). The analysis was carried out by PT Intertek Jakarta and is used to identify trace metals and major elements. The samples in the field were taken by two methods. The seafloor samples were acquired by grab sampler driven above from survey boat and by divers especially in the vicinities of active fumaroles. Another method was by conventional geological sampling through taking samples by a geological hammer from outcrops in a coastal zone. All samples selected for geochemistry were mostly lavas and some pyroclastics and sediments. The sample standard used was sensitive and rapid throughout instrumentation ICP-OES and ICP-MS. Before being analyzed in the instrumentation, the samples were decomposed by applying acid digestion and fusions.

Statistical method is necessary to examine correlation between the individual elements. The statistical method used is correlation coefficient. Correlation coefficient ( $r$ ) is a statistical method to compare two parameters and geologically be interpreted its genesis. Parameters compared are trace and rare earth elements through its content

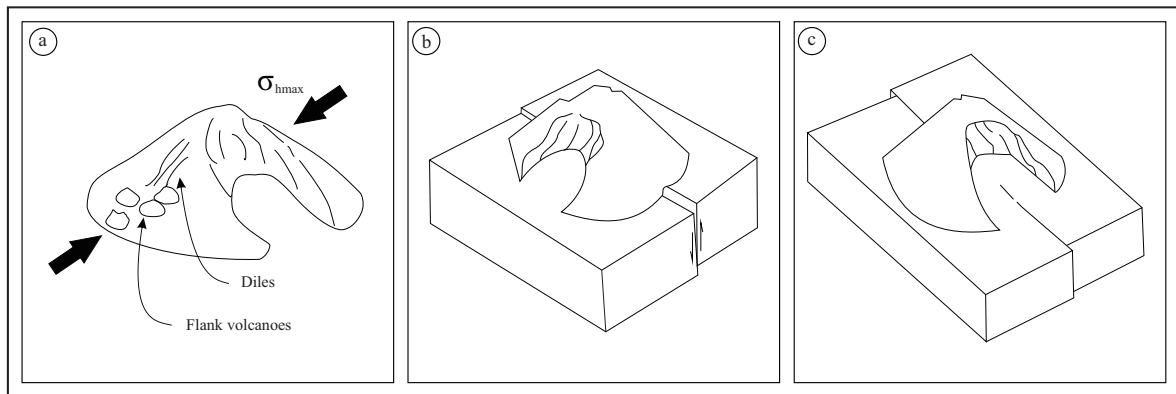


Figure 2. Caldera collapse model based on Lagmay *et al.* (2000): a. The collapse model perpendicular to regional main stress of compressive character. b. The collapse model also perpendicular but to normal fault. c. The collapse model above transform fault parallel to fault movements. The studied area resembles the c model.

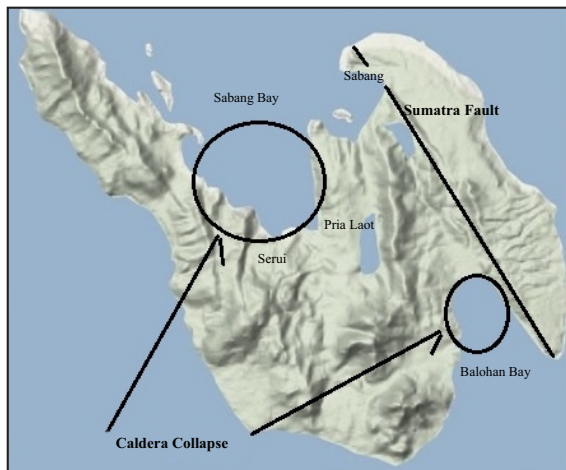


Figure 3. Caldera collapse model of Weh Island which is parallel to horizontal movement of Sumatran Fault is conform with the c model (Lagmay *et al.*, 2000 above).

either in ppm (part per million) or % (percent). The coefisien value closed to 1 (one) means a very good correlation between two parameters or termed as perfect sympathy, closed to 0 (zero)

no correlation and closed to -1 perfect antipathy. Base metal elements such as Cu, Ni, Fe, Zn, Pb, and Mo were also correlated to sulfur (S) to investigate the formation of sulphide minerals. The formula used is from Rollinson (1995):

$$r = \text{CSCP} / \sqrt{(\text{CSSX} \cdot \text{CSSY})}$$

where:

$$\text{CSCP (corrected sum of cross products)} = \sum(xy) - \sum(x) \cdot \sum(y) / n$$

$$\text{CSSX (corrected sum of squares for x)} = \sum(x^2) - \sum(x) \cdot \sum(x) / n$$

$$\text{CSSY (corrected sum of squares for y)} = \sum(y^2) - \sum(y) \cdot \sum(y) / n$$

### RESULTS AND DISCUSSION

The analyses results of rare earth elements (REE) are shown in Table 1. while base metal elements that supposed to form sulphide minerals are presented in Table 2.

Geochemical data of Andaman, Semangko, and Sabang/Weh areas (Table 3) demonstrate

Table 1. Rare Earth Element Contents of Seafloor Fumarole and Coastal Samples (in ppm)

| IDENT                         | Sc  | Y    | La   | Ce   | Pr   | Nd   | Sm   | Eu   | Gd   | Tb     | Dy   | Ho   | Er   | Tm   | Yb   | Lu     |
|-------------------------------|-----|------|------|------|------|------|------|------|------|--------|------|------|------|------|------|--------|
| SERUI - A - 5 M (DIVING)      | 21  | 20.8 | 17.4 | 37.6 | 5.14 | 20.4 | 5    | 1    | 4.2  | 0.63   | 4.4  | 0.9  | 2.3  | 0.4  | 2.2  | 0.83   |
| SERUI - A - 10 M (DIVING) (S) | 10  | 12.3 | 13.7 | 30   | 3.56 | 14.5 | 2.9  | 0.6  | 2.7  | 0.38   | 2.4  | 0.5  | 1.4  | 0.2  | 1.4  | 0.21   |
| SERUI - B - 10 M (DIVING)     | 26  | 24.3 | 14.3 | 30.8 | 4.4  | 18.3 | 4.9  | 1    | 4.7  | 0.75   | 4.1  | 0.9  | 2.6  | 0.4  | 2.5  | 0.41   |
| SERUI - B - 15 M (DIVING) (S) | 15  | 15.3 | 20.2 | 42   | 4.58 | 18.6 | 3.7  | 0.8  | 4    | 0.49   | 3.1  | 0.6  | 1.8  | 0.2  | 1.7  | 0.28   |
| SERUI - C - 10 M (DIVING)     | 30  | 23.5 | 13.9 | 35.2 | 4.78 | 21.8 | 5.5  | 0.9  | 5.2  | 0.73   | 5    | 1    | 2.7  | 0.4  | 2.6  | 0.42   |
| SERUI - C - 23 M (DIVING) (S) | 20  | 16.8 | 15.5 | 35.2 | 4.05 | 17.2 | 4.2  | 0.8  | 4.2  | 0.55   | 3.4  | 0.7  | 1.9  | 0.3  | 1.8  | 0.29   |
| SERUI - D - (DIVING)          | 29  | 26.5 | 17.7 | 39   | 4.78 | 21.8 | 5.3  | 0.9  | 5.3  | 0.69   | 4.8  | 1    | 2.6  | 0.4  | 2.5  | 0.37   |
| SERUI - E - (DIVING)          | 1   | 0.8  | 0.6  | 1.5  | 0.17 | 0.7  | 0.1  | 0.05 | 0.2  | 0.0025 | 0.1  | 0.05 | 0.05 | 0.05 | 0.1  | 0.0025 |
| KPW 01                        | 13  | 15.9 | 19.1 | 42.4 | 4.92 | 19   | 4    | 0.8  | 3.8  | 0.46   | 3.1  | 0.6  | 1.8  | 0.3  | 1.7  | 0.31   |
| KPW 02                        | 15  | 16   | 18   | 39.2 | 4.51 | 16.7 | 3.9  | 0.8  | 3.5  | 0.48   | 3    | 0.6  | 1.7  | 0.3  | 1.7  | 0.31   |
| KPW 03                        | 0.5 | 0.7  | 0.4  | 0.7  | 0.09 | 0.3  | 0.05 | 0.05 | 0.05 | 0.0025 | 0.05 | 0.05 | 0.05 | 0.05 | 0.05 | 0.0025 |
| KPW 07                        | 16  | 15.8 | 21   | 50.3 | 5.2  | 19.2 | 4.1  | 1    | 4.2  | 0.53   | 3.3  | 0.6  | 1.7  | 0.3  | 1.8  | 0.28   |
| KPW 08                        | 17  | 17.6 | 19.7 | 46.4 | 5.43 | 20.7 | 4.7  | 1.1  | 4.2  | 0.56   | 3.6  | 0.7  | 2.1  | 0.3  | 2    | 0.32   |
| KPW 09                        | 12  | 15.9 | 22.9 | 48.1 | 6.13 | 23.2 | 4.6  | 1    | 4.1  | 0.52   | 3.2  | 0.6  | 1.8  | 0.3  | 1.8  | 0.32   |
| KPW 10                        | 21  | 16.1 | 10.7 | 25.3 | 3.02 | 12.2 | 2.9  | 0.8  | 2.9  | 0.46   | 3.1  | 0.7  | 1.8  | 0.3  | 1.9  | 0.3    |
| KPW 11                        | 13  | 15.9 | 20.8 | 43.9 | 5.04 | 18.8 | 4    | 0.9  | 4    | 0.48   | 3.1  | 0.6  | 1.6  | 0.3  | 1.7  | 0.28   |
| KPW 12                        | 16  | 18.5 | 17.1 | 41   | 4.37 | 16.9 | 3.9  | 1    | 3.5  | 0.55   | 3.1  | 0.7  | 2.1  | 0.3  | 1.9  | 0.31   |

Sabang Submarine Volcano Aceh, Indonesia: Review of Some Trace and Rare Earth Elements Abundances Produced by Seafloor Fumarole Activities (H. Kurnio *et al.*)

Table 2. Eight Elements Forming Sulphide Minerals and Barium (Ba) Contents at Seafloor and Coastal Area (in ppm)

| IDENT                         | Cu  | Fe   | Zn | Pb | Ni | As | Mo  | S    | Ba  |
|-------------------------------|-----|------|----|----|----|----|-----|------|-----|
| KPW 01                        | 107 | 4.43 | 65 | 18 | 12 | 34 | 0.9 | 350  | 280 |
| KPW 02                        | 49  | 4.24 | 68 | 18 | 10 | 19 | 0.8 | 230  | 334 |
| KPW 07                        | 54  | 4.3  | 75 | 19 | 11 | 15 | 0.7 | 490  | 463 |
| KPW 08                        | 67  | 4.69 | 74 | 19 | 14 | 20 | 0.7 | 260  | 358 |
| KPW 09                        | 111 | 3.8  | 63 | 20 | 10 | 34 | 0.9 | 570  | 385 |
| KPW 10                        | 39  | 5.37 | 96 | 10 | 16 | 10 | 0.4 | 210  | 212 |
| KPW 11                        | 16  | 4.13 | 69 | 19 | 9  | 11 | 0.7 | 670  | 292 |
| KPW 12                        | 45  | 4.79 | 86 | 18 | 12 | 11 | 0.5 | 940  | 499 |
| SERUI - B - 15 M (DIVING) (S) | 14  | 3.3  | 60 | 19 | 10 | 63 | 3.2 | 6630 | 261 |
| SERUI - C - 23 M (DIVING) (S) | 13  | 3.73 | 66 | 15 | 12 | 16 | 4.6 | 3090 | 171 |

Table 3. Trace and Rare Earth Element Contents of Volcanics and Sediments (in ppm) of Weh, Andaman, and Semangko Islands

| OXYDE/<br>ELEMENT | ANDAMAN<br>(Ray <i>et al.</i> , 2012) |        | SEMANGKO<br>(Kurnio <i>et al.</i> ,<br>2005) | WEH ISLAND |                |          |           |
|-------------------|---------------------------------------|--------|--|------------|----------------|----------|-----------|
|                   | Narcondam                             | Barren | n = 15                                       | Seabottom  | Mineralization | Coast    | Fumaroles |
|                   | n = 10                                | n = 10 |  | n = 14     | n = 14         | n = 12   | n = 10    |
| Sc                | 18.62                                 | 30.68  | 17.6   | 6.0357143  | 7.785714286    | 11.875   | 20.5      |
| V                 | 134.74                                | 249.6  | 117.3333                                     | 87.142857  | 87.57142857    | 122.75   | 183       |
| Cr                | 26.78                                 | 246.51 | 28.56667                                     | 15.857143  | 13.75          | 16.16667 | 16        |
| Co                | 16.46                                 | 27.28  | 21.33333                                     | 7.1071429  | 1.928571429    | 11.625   | 16.25     |
| Ni                | 16.36                                 | 97.33  | 11.23333                                     | 9          | 3.071428571    | 9.5      | 13.3      |
| Cu                | 36.56                                 | 58.23  | 92.6   | 5.2142857  | 6.142857143    | 64.41667 | 25        |
| Zn                | 42.42                                 | 69.03  | 205.8667                                     | 38.071429  | 12.14285714    | 56.08333 | 79.2      |
| Rb                | 44.29                                 | 7.83   | 40.93333                                     | 17.478571  | 40.37857143    | 69.7     | 31.85     |
| Sr                | 267.8                                 | 155.62 | 185.8  | 3777.4286  | 191.1071429    | 752.85   | 659.16    |
| Y                 | 18.29                                 | 23.88  | 11.73333                                     | 6.7857143  | 3.142857143    | 12.56667 | 16.99     |
| Zr                | 49.35                                 | 67.76  | 94.26667                                     | 14.892857  | 48.61428571    | 66.075   | 46.42     |
| Nb                | 2.56                                  | 0.82   | 2  | 1.3        | 2.410714286    | 3.3125   | 4.33      |
| Ba                | 312.64                                | 71.41  | 137.4667                                     | 56.428571  | 218.6428571    | 259      | 116.7     |
| La                | 12.69                                 | 3.86   | 13.33333                                     | 5.0071429  | 15.03571429    | 13.975   | 16.52     |
| Ce                | 21.03                                 | 9.72   | 15.13333                                     | 11.071429  | 30.1           | 31.4     | 38.82     |
| Pr                | 2.67                                  | 1.45   | 25   | 1.4457143  | 3.142857143    | 3.617583 | 4.907     |
| Nd                | 11.01                                 | 7.67   | 11.16667                                     | 6.05       | 10.28571429    | 13.80833 | 19.15     |
| Sm                | 2.57                                  | 2.42   | 3.1  | 1.3964286  | 1.642857143    | 3.025    | 4.04      |
| Eu                | 0.9                                   | 0.88   | 0.953333                                     | 0.3035714  | 0.346428571    | 0.704167 | 0.745     |
| Gd                | 2.99                                  | 3.15   | 0  | 1.3178571  | 1.653571429    | 2.841667 | 3.95      |
| Tb                | 0.45                                  | 0.55   | 0.303333                                     | 0.1892857  | 0.160714286    | 0.387083 | 0.5315    |
| Dy                | 2.83                                  | 3.77   | 0  | 1.2321429  | 0.746428571    | 2.425    | 3.38      |
| Ho                | 0.51                                  | 0.69   | 0  | 0.2464286  | 0.142857143    | 0.495833 | 0.675     |
| Er                | 2.98                                  | 4.08   | 0  | 0.6964286  | 0.389285714    | 1.395833 | 1.875     |
| Tm                | 0.28                                  | 0.39   | 0  | 0.125      | 0.071428571    | 0.2375   | 0.28      |
| Yb                | 1.75                                  | 2.47   | 2.786667                                     | 0.6607143  | 0.403571429    | 1.391667 | 1.75      |
| Lu                | 0.28                                  | 0.39   | 0.407667                                     | 0.1053571  | 0.07           | 0.23625  | 0.3355    |
| Hf                | 1.31                                  | 1.59   | 2.233333                                     | 0.5428571  | 1.482142857    | 1.979167 | 1.485     |
| Ta                | 0.16                                  | 0.07   | 0.25   | 0.2107143  | 0.198571429    | 0.27875  | 0.2755    |
| Pb                | 6.7                                   | 1.99   | 33.49447                                     | 5.4285714  | 14.57142857    | 13.5     | 13        |
| Th                | 4.04                                  | 0.58   | 7.5  | 1.8157143  | 5.601428571    | 7.100833 | 6.432     |
| U                 | 0.96                                  | 0.15   | 2.233333                                     | 1.6371429  | 1.747857143    | 2.071667 | 4.335     |

abundances of elements and oxydes. In Sabang, the abundances occur at some locations closed to fumaroles. Mineralization activities could be observed at Pria Laot coast, while fumaroles noticed by divers occur at a shallow sea of Serui (sea depths 5 to 23 m) and Pria Laot (sea depth less than 10 m). In the vicinities of seafloor fumaroles (sample code using SERUI - (DIVING) in Table 1), trace and rare earth elements such as Nb (4.33 ppm), La (16.52 ppm), Ce (38.82 ppm), Nd (19.15 ppm), Ce (38.82 ppm), Pr (4.907 ppm), Nd (19.15 ppm), Sm (4.04 ppm), Gd (3.95 ppm), Dy (3.38 ppm), Th (6.432 ppm), and U (4.335 ppm) are calculated. The lanthanum (La) content closed to seafloor fumaroles has a mean value of 16.52 ppm, more abundant than that at mineralization zone of Pria Laot (15.0357 ppm), coastal samples surround Weh Island (13.975 ppm), and other seafloor samples (5.007 ppm). The lanthanum content of Weh Island is also higher when compared to that of Andaman volcanic rocks (Table 3). Volcanic rocks from the Semangko Bay, southeast of Sumatra, has a lower value of lanthanum (13.33 ppm) compared to sample from Weh Island.

Andaman and Semangko are used for a comparison as these two locations are located at the same Sunda volcanic belt. Some trace and rare earth elements of Semangko show higher contents than Weh and Andaman Islands possibly due to different tectonic setting, where Semangko is more related to transition of oblique and frontal subduction zone between Sumatra and Java, while the latter islands are located in the middle of oblique subduction Sumatra.

The data show that fumarole activities either on seafloor or on coastal zone contain more abundant trace and rare earth elements. This view was based on the analyses of geophysical data - shallow marine seismics (Figure 4a) and geochemical analyses of rocks and sediments especially obtained from seafloor in the vicinities of active and non-active fumaroles (Figure 4b). Geochemical data of active fumaroles is shown in Table 1 as indicated by sample numbers SERUI - (DIVING).

An interesting phenomenon was observed at the seafloor closed to active fumaroles. In the rim of fumarole vent there is an encrustation of white colour materials (Figure 5a). according to Gilbert and Williams-Jones (2008) these materials are rare earth elements (Figure 5b). Data on REE contents of fumarole vent of Weh Island and its comparison is shown in Table 4.

Statistical analyses were conducted for all rare earth elements by calculation of coefficient correlation for each pair of elements. Example of calculation is shown in Table 5, and all the calculation results are demonstrated in Table 6.

The result shows that the *r* value of *Y versus La* is 0.746635. This significant *r* value could be interpreted that the occurrence of rare earth element *Y* at submarine volcano environment is associated with La. It means that the increased of *Y* element in a volcanic product resulted from seafloor fumarole activities would be followed by increased of La content. All *r* calculation for REE was done through pair by pair of rare earth (Table 6). Based on these all REE coefficient correlation calculations from samples taken in the vicinities

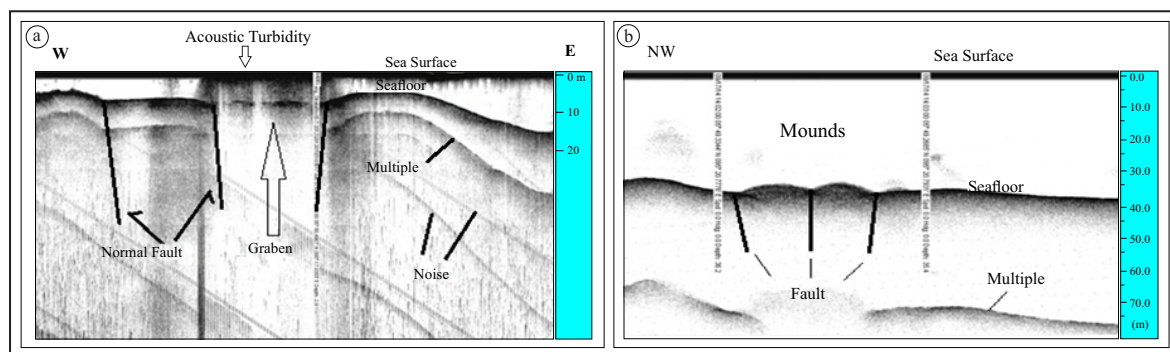


Figure 4. Active fumarole (a) and non-active fumaroles (b) that formed mounds or small highs, interpreted as chimney.

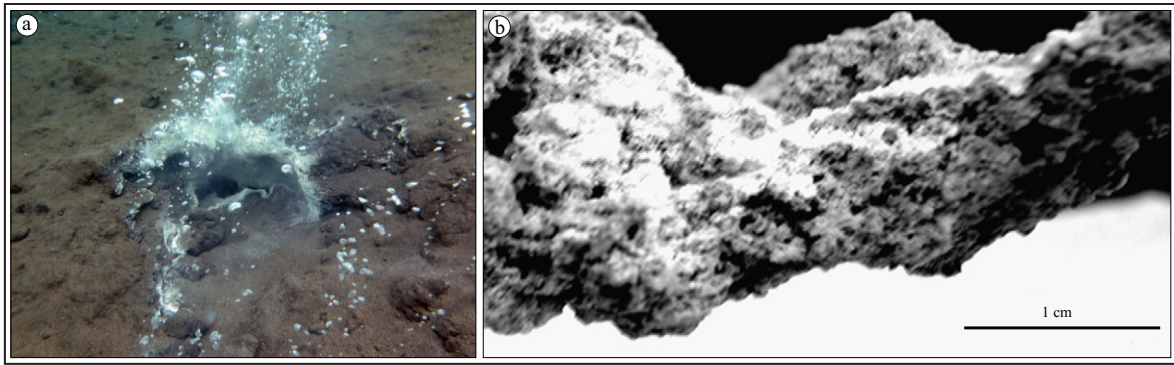


Figure 5. Encrustation surround active seafloor vent in Sabang (a) and encrustation of lava by rare earth element in Oldoinya Lengai (Gilbert and William-Jones, 2008).

Table 4. Comparison of Eight Elements Forming Sulphide Minerals and Barium (Ba) between Sabang (SERUI-B-10M (DIVING)) and Oldoinya Lengai (S4) (Gilbert and Williams-Jones, 2008)

| IDENT                     | Sc  | Y    | La   | Ce   | Pr   | Nd   | Sm   | Eu   | Gd  | Tb   | Dy  | Ho  | Er  | Tm  | Yb  | Lu   |
|---------------------------|-----|------|------|------|------|------|------|------|-----|------|-----|-----|-----|-----|-----|------|
| SERUI - B - 10 M (DIVING) | 26  | 24.3 | 14.3 | 30.8 | 4.4  | 18.3 | 4.9  | 1    | 4.7 | 0.75 | 4.1 | 0.9 | 2.6 | 0.4 | 2.5 | 0.41 |
| S4                        | <dl | 18   | 1320 | 1350 | 96.3 | 218  | 15.2 | 2.96 | 4.7 | 0.5  | 2.2 | 0.4 | 1   | <dl | 0.5 | 0.05 |

Note: <dl = below detection limit

Table 5. Example of r Calculation between Y (as x) and La (as y)

| Y                | La  | x <sup>2</sup>       | y <sup>2</sup>       | x.y                  |
|------------------|---|----------------------|----------------------|----------------------|
| ppm              | ppm                                       |                      |                      |                      |
| 16.8             | 17.4                                      | 282.24               | 302.76               | 292.32               |
| 17.4             | 14.7                                      | 302.76               | 216.09               | 255.78               |
| 0.3              | 0.5                                       | 0.09                 | 0.25                 | 0.15                 |
| 0.3              | 0.5                                       | 0.09                 | 0.25                 | 0.15                 |
| 0.3              | 0.7                                       | 0.09                 | 0.49                 | 0.21                 |
| 1.8              | 22.6                                      | 3.24                 | 510.76               | 40.68                |
| 15.9             | 19.1                                      | 252.81               | 364.81               | 303.69               |
| 16               | 18  | 256                  | 324                  | 288                  |
| 15.8             | 21  | 249.64               | 441                  | 331.8                |
| 17.6             | 19.7                                      | 309.76               | 388.09               | 346.72               |
| 15.9             | 22.9                                      | 252.81               | 524.41               | 364.11               |
| 16.1             | 10.7                                      | 259.21               | 114.49               | 172.27               |
| 15.9             | 20.8                                      | 252.81               | 432.64               | 330.72               |
| 18.5             | 17.1                                      | 342.25               | 292.41               | 316.35               |
| 0.8              | 0.6                                       | 0.64                 | 0.36                 | 0.48                 |
| 17.4             | 17.2                                      | 302.76               | 295.84               | 299.28               |
| 15.3             | 20.2                                      | 234.09               | 408.04               | 309.06               |
| 16.8             | 15.5                                      | 282.24               | 240.25               | 260.4                |
| $\Sigma x=218.9$ | $\Sigma y=259.2$                          | $\Sigma x^2=3583.53$ | $\Sigma y^2=4856.94$ | $\Sigma x.y=3912.17$ |
| CSCP : 760.01    | $\frac{CSSY}{\sqrt{CSSX.CSSY}}$ : 1124.46 | r : 0.746635         |                      |                      |
| CSSX : 921.4628  |   |                      |                      |                      |

of active seafloor fumaroles, it is interpreted that the REE contents would be increased in ac-

cordance with increasing activity of fumaroles. Furthermore, the r value of Y *versus* La gained

Table 6. Coefficient Correlation of All REE from Seafloor Fumaroles

|    | Sc       | Y        | La       | Ce       | Pr       | Nd       | Sm       | Eu       | Gd       | Tb       | Dy       | Ho       | Er       | Tm       | Yb       | Lu |
|----|----------|----------|----------|----------|----------|----------|----------|----------|----------|----------|----------|----------|----------|----------|----------|----|
| Sc | 1        |          |          |          |          |          |          |          |          |          |          |          |          |          |          |    |
| Y  | 0.950791 | 1        |          |          |          |          |          |          |          |          |          |          |          |          |          |    |
| La | 0.682221 | 0.746635 | 1        |          |          |          |          |          |          |          |          |          |          |          |          |    |
| Ce | 0.737856 | 0.799952 | 0.991991 | 1        |          |          |          |          |          |          |          |          |          |          |          |    |
| Pr | 0.725572 | 0.787861 | 0.991168 | 0.991239 | 1        |          |          |          |          |          |          |          |          |          |          |    |
| Nd | 0.772743 | 0.828948 | 0.981858 | 0.986186 | 0.995135 | 1        |          |          |          |          |          |          |          |          |          |    |
| Sm | 0.845049 | 0.887172 | 0.949922 | 0.968047 | 0.974086 | 0.995135 | 1        |          |          |          |          |          |          |          |          |    |
| Eu | 0.858537 | 0.89252  | 0.932558 | 0.960504 | 0.959193 | 0.959193 | 0.981758 | 1        |          |          |          |          |          |          |          |    |
| Gd | 0.899875 | 0.946948 | 0.89917  | 0.929831 | 0.921541 | 0.921541 | 0.973519 | 0.955124 | 1        |          |          |          |          |          |          |    |
| Tb | 0.94219  | 0.971985 | 0.860558 | 0.900603 | 0.89296  | 0.89296  | 0.963548 | 0.96315  | 0.985276 | 1        |          |          |          |          |          |    |
| Dy | 0.956141 | 0.991697 | 0.79483  | 0.84251  | 0.833875 | 0.833875 | 0.921368 | 0.919675 | 0.973473 | 0.9852   | 1        |          |          |          |          |    |
| Ho | 0.964402 | 0.994553 | 0.694648 | 0.752244 | 0.741958 | 0.741958 | 0.856947 | 0.864316 | 0.925772 | 0.958539 | 0.985173 | 1        |          |          |          |    |
| Er | 0.947387 | 0.995732 | 0.743302 | 0.797554 | 0.784665 | 0.784665 | 0.884601 | 0.890948 | 0.94287  | 0.969806 | 0.987947 | 0.992608 | 1        |          |          |    |
| Tm | 0.927524 | 0.981375 | 0.709758 | 0.76808  | 0.760967 | 0.760967 | 0.860889 | 0.864848 | 0.919428 | 0.943577 | 0.972337 | 0.97698  | 0.969428 | 1        |          |    |
| Yb | 0.949721 | 0.987819 | 0.733762 | 0.784972 | 0.776793 | 0.776793 | 0.871544 | 0.884942 | 0.93197  | 0.956273 | 0.983286 | 0.982087 | 0.983232 | 0.969212 | 1        |    |
| Lu | 0.922294 | 0.982817 | 0.729383 | 0.77698  | 0.76941  | 0.76941  | 0.859243 | 0.863129 | 0.922707 | 0.941103 | 0.973769 | 0.97274  | 0.979532 | 0.970369 | 0.992876 | 1  |

Notes: all coefficient are significant

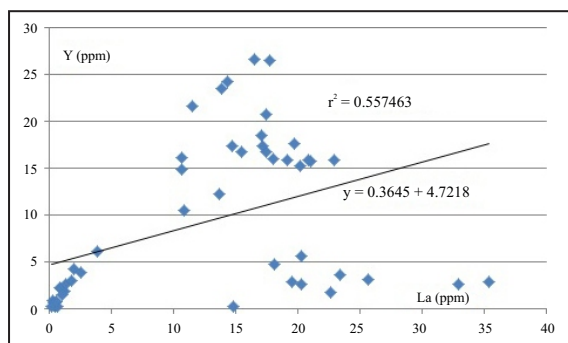


Figure 6. Regressive correlation diagram showing a strong positive correlation between Y and La.

from the formulated calculation (0.746635) is confirmed with the  $r = 0.746634$  ( $r^2 = 0.557463$ ) presented in Figure 6. This figure also tends to

indicate that a strong positive correlation occurs between Y and La.

Base metal elements (Table 2) which form sulphide minerals with sulphur were also correlated. The results (Table 7 and Figure 7) demonstrate that four base metals, those are Fe, Zn, Ni, and Mo, are moderate to strong correlated with sulphur (S), whilst the four rest elements (As, Ba, Cu, and Pb) show very weak to moderate correlations with S. Table 7 and Figure 7 display that only two elements, those are Mo ( $r = 0.561$ ) situated within a significant moderate positive correlation with S, and Pb within a weak positive correlation ( $r = 0.396$ ). On the contrary, S has a strong negative correlation with Fe ( $r = 0.60$ ), moderate negative

Table 7. Coefficient Correlation of Sulphide Elements and Barium

|    | Ba       | Cu       | Fe       | Zn       | Pb       | Ni       | As       | Mo       | S |
|----|----------|----------|----------|----------|----------|----------|----------|----------|---|
| Ba | 1        |          |          |          |          |          |          |          |   |
| Cu | 0.392571 | 1        |          |          |          |          |          |          |   |
| Fe | 0.630121 | 0.340159 | 1        |          |          |          |          |          |   |
| Zn | 0.702466 | 0.309265 | 0.95519  | 1        |          |          |          |          |   |
| Pb | 0.8638   | 0.415863 | 0.672732 | 0.765831 | 1        |          |          |          |   |
| Ni | 0.543213 | 0.287803 | 0.939565 | 0.950619 | 0.651812 | 1        |          |          |   |
| As | 0.238042 | 0.640296 | 0.194853 | 0.168404 | 0.372968 | 0.146739 | 1        |          |   |
| Mo | -0.15798 | -0.2286  | -0.30266 | -0.15275 | 0.098086 | -0.11713 | 0.138815 | 1        |   |
| S  | -0.37033 | -0.30921 | -0.60079 | -0.58563 | -0.3966  | -0.54058 | 0.098788 | 0.561766 | 1 |

Notes: red positive correlation significant, green negative correlation significant



Sabang Submarine Volcano Aceh, Indonesia: Review of Some Trace and Rare Earth Elements Abundances Produced by Seafloor Fumarole Activities (H. Kurnio *et al.*)

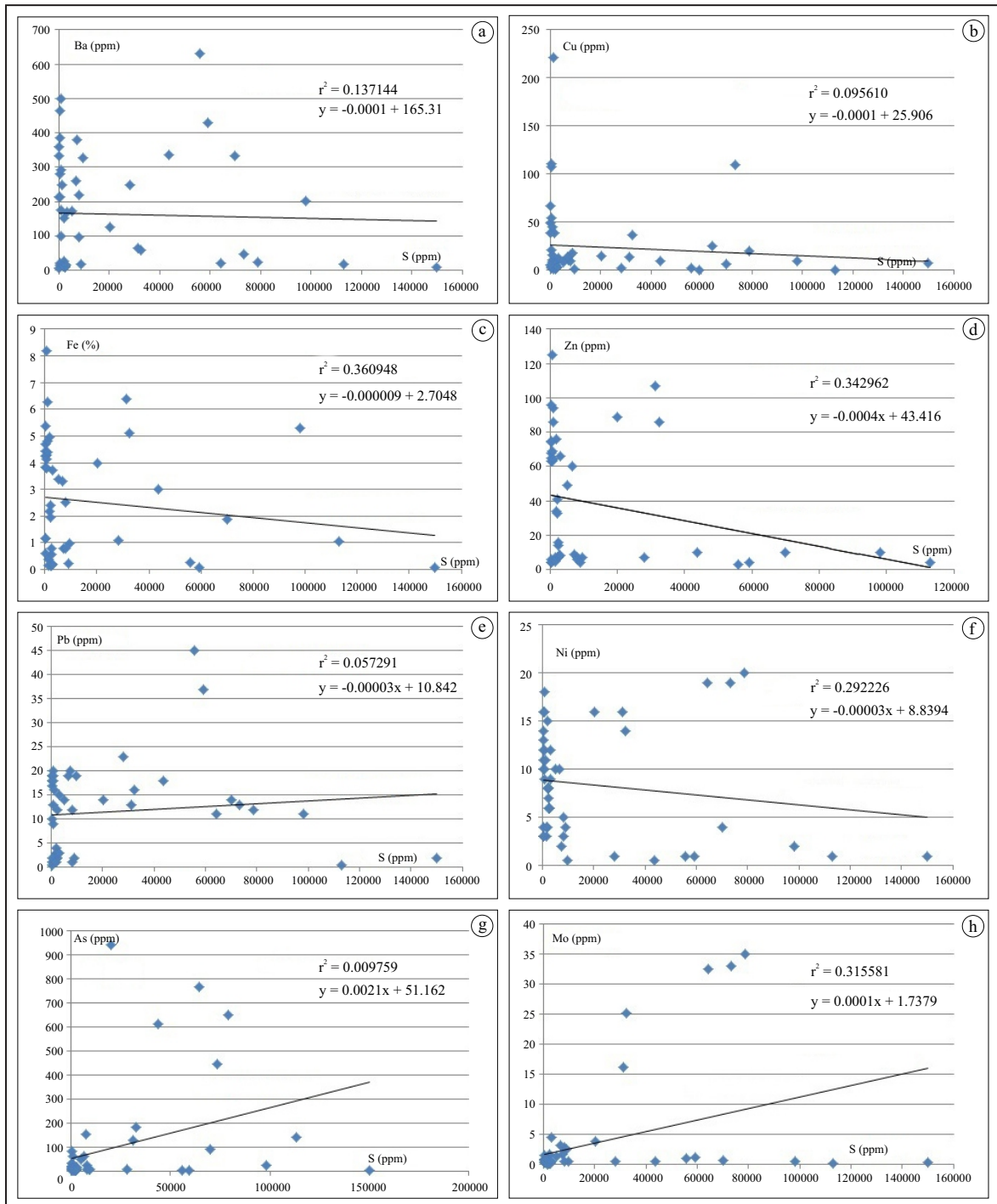


Figure 7. Regressive correlation diagram of: a. S vs. Ba, b. S vs. Cu, c. S vs. Fe, d. S vs. Zn, e. S vs. Pb, f. S vs. Ni, g. S vs. As, and h. S vs. Mo.

correlation with Zn ( $r = 0.586$ ) and Ni ( $r = 0.540$ ), and weak negative correlation with Ba ( $r = 0.370$ ) and Cu ( $r = 0.310$ ). It is interpreted that sulphide minerals are not well developed in the study area. The influence of sea water in the mineralisation process was also investigated through statistic

analyses correlating barium (Ba) with base metals (Shellabear, 2012). Ba is only well concomittant with Fe, Zn, Pb, and Ni (Table 7).

The correlation among elements of REE will be discussed further by utilizing spider diagram as shown in Figure 8. This diagram is used to

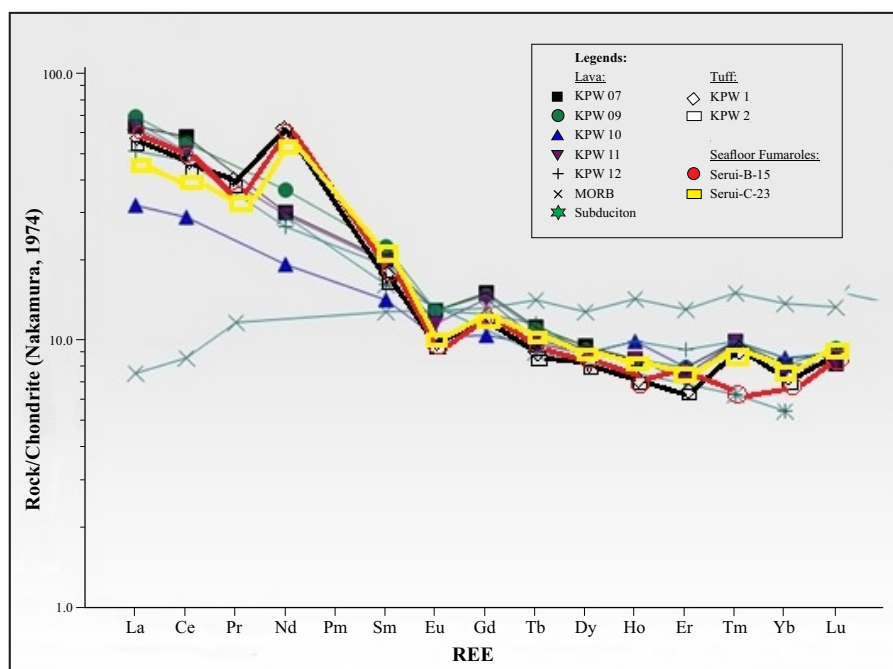


Figure 8. Weh Island spider diagram. The highly fluctuative composition is a characteristic of calk-alkaline magma series of subduction zone (Rollinson, 1995). REE composition was normalized to MORB (Source: www.tulane.edu).

analyze tectonic setting of the study area. The REE average composition at the study area was normalized to the composition of Mid-Oceanic Ridge Basalt (MORB). Contents of some rare earth elements are high. such as: Y=21.6 ppm; Dy=4.5 ppm; Gd=4.3 ppm; Nd=19.9 ppm; Sm=5 ppm. and Yb=2.4 ppm. Figure 8 also shows that the content of light rare earth elements (LREE) are much higher than the contents of Mid-Oceanic Ridge Basalt; while the heavy rare earth elements (HREE) are lower. This spider diagram pattern resembles to geochemical characteristics of subduction zone which is composed of magma series calk-alkaline (Rollinson. 1995). All those samples used for analyses of REE provenance are andesitic lava, tuff, and sand sediments enriched in andesitic fragments taken from the vicinities of seafloor fumaroles.

### CONCLUSION AND SUGGESTION

All the rare earth elements (REE) were interpreted to form in the same process of deposition by fumaroles surrounding the craters which could be either active or non-active.

On the other hand, sulphide minerals do not form in the Sabang water, because there is no correlation between Fe, Zn, and Ni as the main sulphide elements with sulphur. All are statistically negatively correlated. Well correlations between Fe, Zn, Pb, Ni, and Ba is interpreted to be due to sea water influence in the mineralization process.

### ACKNOWLEDGEMENTS

The authors would like to thank the Director of Marine Geological Institute for supporting to attend the AOGS 2015 Annual meeting in Singapore. This paper has been presented at the AOGS event.

### REFERENCES

Barber, A.J., Crow. M.J., and Milsom. J.S. (Eds.), 2005. Sumatra. Geology, Resources and Tectonic Evolution. *Geological Society, London. Memoirs*, 31. DOI: 10.1144/GSL.MEM.2005.031.01.19.

- Bellier, O. and Sebrier, M., 1994. Relationship between tectonism and volcanism along the Great Sumatran fault zone deduced by SPOT image analyses. *Tectonophysics*, 233, p.215-231. DOI: 10.1016/0040-1951(94)90242-9
- Crow, M.J. and Barber, A.J. (Eds.), 2005. Simplified geological map of Sumatra. *Geological Society, London, Memoirs*, 31. DOI: 10.1144/GSL.MEM.2005.031.01.19.
- Curry, J., Moore, D., Lawyer, L., Emmel, F., Raitt, R., Henry, M., and Kieckhefer, 1979. Tectonics of the Andaman Sea and Burma. *AAPG Memoir*, 29, p.189-198.
- Curry, J.R., 2005. Tectonics and history of the Andaman Sea region. *Journal of Asian Earth Sciences*, 25 (1), p.187-232. Bibcode:2005JAESc.25.187C.
- Dirasutisna, S. and Hasan, A.R., 2005. Geologi Panas Bumi Jaboi, Sabang, Propinsi Aceh Nangroe Darussalam. *Direktorat Inventarisasi Sumber Daya Mineral*, Bandung.
- Gilbert, C.D. and Williams-Jones, A.E., 2008. Vapour transport of rare earth elements (REE) in volcanic gas: Evidence from encrustations at Oldoinya Lengai. *Journal of Volcanology and Geothermal Research*, 176, p.519-528. DOI: 10.1016/j.jvolgeores.2008.05.003
- Heinrich, C.A., Gunther, D., Audetat, A., Ulrich, T., and Frischnecht, R., 1999. Metal fractionation between magmatic brine and vapour. determined by microanalyses of fluid inclusions. *Geology*, 27 (8), p.255-258.
- Kurnio, H., Schwarz-Schampera, U., and Wiedecke-Hombach, M., 2005. Tabuan Island, Indonesia. Subaerial Hydrothermal Mineralization on Tabuan Island, Semangko Bay, South Sumatra, Indonesia. *BGR - Bundesanstalt für Geowissenschaften und Rohstoffe*. Hannover, Tgb.-Nr.: 10708/05.
- Lagmay, A.M.F., de Vries, van Wyk, B., Kerle, N., and Pyle, D.M., 2000. Volcano instability induced by strike-slip faulting. *Bulletin of Volcanology*, 62, p.331-346. DOI: 10.1007/s00450000103.
- Ray, D., Rajan, S., and Ravindra, R., 2012. Role of subducting component and sub-arc mantle in arc petrogenesis: Andaman volcanic arc. *Current Science*, 102 (4), p.605-609.
- Rollinson, 1995. *Using geochemical data: evaluation, presentation, interpretation*. Longman Singapore Publishers (Pte) Ltd.. 352pp.
- Shellabear, J., 2012. Exploration Update. Girilambone Copper/Gold Project. Heron Resources Limited. ABN: 30 068 263 098. Level1. 37 Ord Street. West Perth WA 6005.
- Sieh, K. and Natawidjaja, D., 2000. Neotectonics of the Sumatran fault. Indonesia. *Journal of Geophysical Research*, 105 ( B12), p.28.295 - 28.326. DOI: 10.1029/2000JB900120
- Simoës, M., Avouac, J.P., Cattin, R., and Henry, P., 2004. "The Sumatra subduction zone: A case for a locked fault zone extending into the mantle" (PDF). *Journal of Geophysical Research*, 109 (B10402). Bibcode:2004JGRB..10910402S. DOI: 10.1029/2003JB002958
- Suhanto, E., Sriwidodo, Munandar, A., Kusnadi, D., and Kusuma, D.S., 2005. Penyelidikan terpadu geologi, geokimia, dan geofisika daerah panas bumi Jaboi, Kota Sabang - Nangroe Aceh Darussalam. *Pemaparan Hasil Kegiatan Survei Panas Bumi*. Pusat Sumber Daya Geologi (PSDG) Badan Geologi, 63pp.
- Tikoff, B., 1998. Sunda-style tectonics and magmatic arc processes. *Eos Trans. AGU*, 79 (45), Fall Meet. Suppl., F222.
- Tim Geomarin I, 2011. Pemetaan Geologi dan Geofisika Kelautan Dengan Kapal Geomarin I Perairan LP 0421 (Perairan Aceh Utara). *LAPORAN. Puslitbang Geologi Kelautan*, tidak terbit.
- Williams-Jones, A.E., Migdisov, A.A., Archibald, S.M., and Xiao, Z., 2002. Vapour transport of ore metals. In: Hellman, R. and Wood, S.A. (Eds.), *Water-Rock Interactions, Ore Deposits. and Environmental Geochemistry: A Tribute to David A Crerar*. Special Publication, 7. The Geochemical Society, p.279-305.